Journal of Food Engineering 410 (2026) 112934

Contents lists available at ScienceDirect

Journal of Food Engineering

journal homepage: www.elsevier.com/locate/jfoodeng

Development and characterization of foam-mat freeze-dried beetroot powders: Role of carrier agents in foam behavior, powder functionality, and tablet formation

Vamsi Pavan Kumar Boddapati [a], Sareena Vanchipurackal Sherif [a], Jabbar Gardy [b], Ali Hassnapour [c], Rammile Ettelaie [d], Amin Farshchi [a,*]

[a] School of Health and Life Sciences, Teesside University, TS1 3BX, UK
[b] Cormica Bradford Limited, Listerhills Science Park, Campus Road, Bradford, BD7 1HR, UK
[c] School of Chemical and Process Engineering University of Leeds, LS2 9JT, UK
[d] Food Colloids Group, School of Food Science and Nutrition, University of Leeds, LS2 9JT, UK

ARTICLE INFO

Keywords:
Beetroot powder
Foam-mat freeze drying
Powder functionality
Tablet formation
Maltodextrin
Xanthan gum

ABSTRACT

This study investigates the development of foam-mat freeze-dried beetroot powders and examines the role of carrier agents, maltodextrin and xanthan gum, on powder functionality and tablet formation. All formulations contained egg white albumen (5 wt%) as a foaming agent, while compositions varied based on the presence of maltodextrin (5 wt%) and xanthan gum at various concentrations (0.05, 0.1, or 0.2 wt%). Foams were prepared by whipping beetroot juice mixtures, followed by freeze-drying. The addition of maltodextrin slightly improved foam expansion (from ~450 % to ~460 %) and foam stability, whereas xanthan gum significantly increased the foam stability, with no drainage observed at 0.1 and 0.2 wt% within 180 min. However, foam expansion decreased to ~370 % at 0.2 wt% xanthan gum content. Maltodextrin improved flowability (Hausner Ratio, HR: 1.29 vs. 1.32 for control) and reduced hygroscopicity (23.5 % vs. 26.0 %), while xanthan gum increased particle irregularity and cohesiveness, thus leading to higher HR values (up to 1.47) and poorer flow. The inclusion of xanthan gum also reduced powder solubility from ~92 % down to ~77 %. Kawakita analysis showed that maltodextrin and xanthan gum reduced plastic deformation and powder compactness. Tablets prepared from these powders exhibited reduced tensile strength and density compared to the control. Color analysis indicated that carrier addition increased lightness (L*) and decreased redness (a*), primarily due to pigment dilution and reduced compactness.

1. Introduction

Freeze drying is an excellent dehydration technique widely used for preserving heat-sensitive functional foods, and encapsulating thermolabile bioactive compounds and pigments (Akbarbaglu et al., 2024; Kandasamy and Naveen, 2022; Qadri et al., 2020). The increasing use of encapsulated plant-based pigments in food production has shown a remarkable growth in recent years, largely due to consumer concerns about the health risks associated with synthetic food colorings (Jurić et al., 2022). Betalains, a class of water-soluble nitrogen-containing pigments found in red beetroot (*Beta vulgaris* rubra, BVr), are particularly noteworthy in this context. These pigments, including betacyanins (red-violet) and betaxanthins (yellow-orange), are used as natural colorants in various foods due to their pH stability and strong antioxidant properties (Kerr and Varner, 2020; Pitalua et al., 2010; Ninfali and Angelino, 2013; Shakir and Simone, 2024). Despite their benefits, betalains are unstable during processing conditions involving light, oxygen, and high temperatures (Tekin et al., 2023).

Freeze drying offers an effective method to encapsulate these pigments, enhancing their stability and usability as natural food colorants or functional additives. However, freeze drying is a slow and energy-intensive process, making it more expensive than other dehydration methods such as spray drying (Stapley, 2008). To address this limitation, liquid foods can be foamed by vigorous whipping or injecting gas through a sparger. The resulting foamed structure increases the surface area between the gas–liquid interface and the drying medium (air or

* Corresponding author.
E-mail address: a.farshchi@tees.ac.uk (A. Farshchi).

https://doi.org/10.1016/j.jfoodeng.2025.112934
Received 23 July 2025; Received in revised form 11 December 2025; Accepted 15 December 2025
Available online 18 December 2025

vacuum), which enhances both heat and mass transfer during the initial stages of drying. This accelerates moisture removal and reduces overall drying time (A et al., 2015).

Foam-mat drying is an efficient and economical technique to produce food powders, compared to spray and freeze-drying processes, in terms of energy consumption. The process involves incorporating air into a liquid food (during whipping stage) to form stable gas-liquid foams, followed by a drying stage using either freeze drying or air drying, depending on the intended application and product requirements. For the drying step, the foam is spread on trays as a mat and then exposed to drying air or vacuum until the desired moisture content is achieved. The dried foam is then ground to produce powders which typically have porous structures and show easy reconstitution, high retention of nutritional quality and good powder handling and transportation, *e.g.*, powder flowability (Qadri et al., 2020).

Aqueous foams are complex colloidal systems consisting of gas bubbles dispersed within a continuous aqueous matrix, stabilized by surface active additives. However, they are thermodynamically unstable and tend to coarsen and dissipate over time due to the high surface energy of the formed gas-liquid interfaces (Dickinson, 1992). During foam-mat drying, mass diffusion occurs through liquid capillary channels formed in between the packed bubbles, thus making foam stability essential for effective moisture removal (Dehghannya et al., 2018b; Hardy and Jideani, 2017).

Food proteins are widely used as foaming agents for producing stable liquid foams due to their ability to adsorb strongly to the air-water interfaces, forming films with high interfacial elasticity and viscosity. Moreover, they provide good steric and electrostatic stabilization (Murray and Ettelaie, 2004). Egg white (EW) protein is one of the most commonly used ingredients for aeration and foam stabilization with excellent foaming properties (Dickinson, 2011). However, egg white protein-stabilized foams occasionally display poor stability over storage time (Dehghannya et al., 2018a; Muthukumaran et al., 2008; A et al., 2015). Various thickening agents can be added to egg white protein to slow down film drainage (Murray, 2020). Polysaccharides are commonly used to stabilize foams by increasing the viscosity of the continuous phase directly or through formation of gel structures. This slows down the movement of air bubbles, as well as reduces liquid drainage from the space between the bubbles (Dickinson, 1992). Maltodextrin, a polysaccharide composed of glucose units linked by α-1, 4 glycosidic bonds, is commonly used as a stabilizer, thickener, and bulking agent in food and beverage applications due to its good water-solubility and hydrophilic properties (Darniadi et al., 2018).

Xanthan gum, a high molecular weight anionic polysaccharide produced by *Xanthomonas campestris* bacteria, is valued for its unique rheological properties, making it useful in various industries including food, cosmetics, and chemicals (Sanderson, 1981). Xanthan gum can improve the stability of foams by increasing the low-shear viscoelasticity, which again slows down the coalescence of the gas bubbles and the drainage of the liquid phase. Moreover, xanthan gum can interact with other surface-active components in the foam, such as proteins and surfactants, forming a complex network that stabilizes the gas-liquid interface (Mohanan et al., 2020; Narchi et al., 2009). This interfacial stabilization is particularly important during the whipping process of foam-mat drying techniques, where foams must remain stable and retain their open structure before the subsequent drying process (Hardy and Jideani, 2017). When used for encapsulation purposes, xanthan can form a stable and protective matrix around an active ingredient, which helps to improve its stability and bioavailability in powders or dry systems (Ray et al., 2016). Furthermore, significant shear-thinning behavior of xanthan solutions at higher shear rates can be beneficial in the ease of whipping, while still maintaining the large viscosities at lower shears (Martínez-Padilla et al., 2015).

Several studies have investigated the encapsulation of coloring pigments from fruit and vegetable extracts, particularly betalains from red beetroot, using different drying techniques (Čakarević et al., 2020; García-Segovia et al., 2021; Janiszewska, 2014; Ravichandran et al., 2014). However; only limited research has focused on foam-mat drying (Ng and Sulaiman, 2018; Omidi et al., 2024), and even fewer on the foam-mat freeze-drying approach (Hajiaghaei and Sharifi, 2022). While these studies have mainly addressed pigment retention and powder yield, less attention has been given to the downstream functionality of the powders, especially the role of carrier agents such as foam stabilizers on their performance in solid formats, particularly in terms of powder compaction and tableting properties.

Compaction of powders into tablets is well-established in the pharmaceutical industry for producing solid oral dosages, but its application in the food industry remains in the early stages of development (Naji-Tabasi et al., 2021, Saifullah et al., 2014; Wu et al., 2022; Zea et al., 2013). Some vegetable powders, such as beetroot powder are often bulky and highly hygroscopic, requiring careful and expensive handling during storage and transportation. Compressing such powders into a tablet form offers several advantages, including improved physical and chemical stability, reduced hygroscopicity due to the lower exposed surface area, extended shelf life, and a greater ease in storage and their transportation (Naji-Tabasi et al., 2021; Saifullah et al., 2016). To the best of our knowledge, only a few studies have explored the dual role of carrier agents in influencing foaming behavior and powder functionality, and even a smaller number have addressed their impact on the compaction and tableting performance of beetroot powders produced by foam-mat freeze-drying. The present work investigates how maltodextrin and xanthan gum affect foam stability, powder properties (flowability, solubility, hygroscopicity), and compressibility, with particular emphasis on the tableting behavior of the resulting powders. These insights aim to support the design of beetroot-based tablets as natural colorants and functional ingredients for applications in the food and nutraceutical sectors.

2. Materials and methods

2.1. Materials

Organic beetroot juice (11.6 ± 0.5 °Brix total soluble solids, TSS) was purchased from a local supermarket in Middlesbrough, UK. The juice was labelled as containing no added sugar or preservatives. Maltodextrin with dextrose equivalent (DE) value of 17–19, egg white albumen (84.1% protein), and xanthan were purchased from Special Ingredients LTD, UK. The egg white protein was used as a foaming agent, and maltodextrin and xanthan gum were selected as foam stabilizers.

2.2. Preparation of foams

Five beetroot juice samples were prepared by adding the egg white albumen protein and foam stabilizers to the beetroot juices, stirring the mixture with a magnetic bar for 15 min at room temperature. All the juice samples contained egg white protein (5 wt%). However, their formulation varied depending on the addition of maltodextrin (at 5 wt% when added) or xanthan gum (with various addition amounts at 0.05, 0.1 or 0.2 wt%) to the beetroot juice. These formulations are shown in Table 1. To obtain the foam, the samples were transferred to a graduated 1000 mL plastic beaker and whipped using a hand mixer (Vonshef) fitted

Table 1
Formulations of beetroot juice samples.

Sample	Egg White albumen (wt %)	Maltodextrin (wt %)	Xanthan Gum (wt %)
EP	5.00		
EP.M	5.00	5.00	
EP.M.X0.05	5.00	5.00	0.05
EP.M.X0.1	5.00	5.00	0.10
EP.M.X0.2	5.00	5.00	0.20

with a single whisk attachment, at a speed setting of 3 at 20 °C, for 5 min.

2.3. Freeze-drying of foams

The Foamed beetroot juice samples were transferred into Petri dishes (internal diameter of 86 mm) and frozen in a blast freezer (Foster, BCF21, UK) at −40 °C for 4 h. The frozen foams were then dried using a laboratory freeze dryer (Martin Christ, Alpha 1-2LD plus, Germany) at −90 °C for 48 h under a vacuum pressure of 1 mbar (main drying). This was followed by a final drying step at −90 °C for 4 h, under a reduced pressure of 0.0015 mbar. After freeze-drying, the samples were ground using a spice grinder and stored in a desiccator at 11 % relative humidity and 21 ± 1 °C for three weeks prior to powder characterizations. This relative humidity was created using a saturated solution of lithium chloride.

2.4. Foam characterisation

2.4.1. Foaming capacity: foam expansion and foam density

Foam expansion reflects the amount of air/gas incorporated into the system during whipping, and was measured immediately after the whipping process. It was calculated using the following equation (Ng and Sulaiman, 2018):

$$\text{Foam expansion } (\%) = \frac{V_1 - V_0}{V_0} \times 100 \quad (1)$$

Where, V_0 is the volume of the initial liquid (before whipping) and V_1 is the volume of the resulting foam.

Foam density was measured according to the method of Allen et al. (2006), with slight modifications. After whipping, samples of beetroot foam were gently scooped from the plastic beaker using a rubber spatula and filled up into a previously weighed beaker, having a volume of 100 mL. The filling was carried out carefully to avoid creating voids and/or destroying the foam structure while transferring the foamed juice into the beaker. The top of the beaker was then levelled with a metal spatula to ensure consistency of the measurements. Foam density is calculated by dividing the measured weight of foam by its volume.

2.4.2. Foam stability: liquid drainage measurements and microscopic observations

Foam stability was measured using a modified procedure based on Chandrakar et al. (2024). It was assessed by monitoring liquid drainage from the foamed beet juice samples, which were gently placed in a 500 mL measuring cylinder. The volume of drained liquid was recorded over a period of 180 min. Microscopic observations were also performed to evaluate foam structure. Foam samples were collected immediately after foam preparation and again after 45 min of standing. A small portion of each sample was carefully placed on a clean glass slide and visualized under a GXM-L2800 microscope (GT Vision, Stanfield, United Kingdom) using a ×4 objective lens.

2.4.3. Foam firmness

The firmness of the foamed beetroot juice samples was assessed using a texture analyzer (Brookfield CT3 Texture Analyzer, Middleboro, MA, USA) equipped with a ball probe (TA43 with a 25.4 mm diameter) and a 4.5 kg load cell (≈44 N), which had a resolution of 0.5 g. The test was conducted in back-extrusion mode. The ball probe was chosen over a conventional flat-plate probe as its rounded shape helps reduce edge effects and localized disturbances during compression in soft materials (Chen et al., 2021). This is particularly important when testing foams where irregular force distribution can affect measurement consistency. Foamed beetroot juice samples were gently transferred into an acrylic cylindrical cup (inner diameter of 25.6 mm, height 30 mm) to ensure that the foam structure remained intact. The containers were filled to a consistent level to provide uniformity across all samples. The ball probe was attached to the instrument, and the test parameters were set as follows: test speed of 1 mm/s and compression distance of 25 mm. The filled containers were placed on the base platform of the texture analyzer, and the ball probe was positioned just above the surface of the foam. The test was initiated, and the probe descended to the specified compression distance. During the test, the force exerted by the probe on the foam was recorded continuously. The maximum force encountered during the compression was recorded and taken as a measure of the firmness of the foam. Each sample was tested in triplicate to ensure accuracy and reproducibility.

2.5. Powder characterisation

2.5.1. Hygroscopicity and moisture sorption properties

The sorption behavior of beetroot powders was gravimetrically determined using a dynamic vapor sorption (DVS) technique (DVS Advantage, Surface Measurement Systems, Middlesex, UK). The samples were loaded in a sample pan (100 μL) and an empty pan was used as a reference. The DVS profiles were obtained by raising relative humidity from 0 % to 70 % RH in increments of 10 % RH steps at 25 °C. At each RH step the sample was allowed to reach a gravimetric equilibrium, when the change in mass (dm/dt) is lower than 0.002 mg/min, and then the sample progressed to the next RH step (Farshchi et al., 2019). The equilibrium moisture content (% E.M.C) on a dry basis, *e.g.*, g H_2O/100 g solids of the samples determined at 70 % RH, was used to assess the hygroscopic characteristics of the beetroot powders.

2.5.2. Solubility index measurements

Instant reconstitution of food powders is a crucial attribute for ensuring high-quality consumption experiences. The rehydration or reconstitution process for these powders typically involves sequential phases: initial wetting (wettability), submersion (sinkability), dispersion (dispersibility), and finally, dissolution (solubility) (Ren et al., 2024). Solubility is the final step in powder reconstitution and, therefore, a key physical property that determines the overall reconstitution quality of food powders (Fang et al., 2007). In this study, solubility was determined according to a method described by Darniadi et al. (2018) with slight modifications. The powder sample (1.0 g) was dissolved in 50 mL distilled water at 20 ± 1 °C, and stirred with magnetic stirrer at 500 rpm for 5 min. The suspensions were then transferred to centrifuge tubes (2×25 mL) and centrifuged at 4500 rpm for 5 min. Aliquots of 10 mL of the supernatant were transferred to aluminium pans and dried in an oven at 105 °C for 24 h. After drying, solubility index was calculated as the ratio of solids in the dried supernatant to the dry weight of the initial sample, Eq. (2).

$$\text{Solubility index} = \frac{\text{weight of dissolved solids in supernatant}}{\text{weight of initial sample}} \times 100 \quad (2)$$

2.5.3. Bulk density measurement and flowability assessment

The flowability of the beetroot powder was assessed through the determination of bulk density, tapped density, Hausner ratio (HR), and Carr's index (Seerangurayar et al., 2017). For bulk density measurements, a known weight of the beetroot powder was carefully poured into a 50.0 mL measuring cylinder through a funnel positioned at a fixed height to ensure a consistent pour. The initial volume of the powder was recorded as the bulk volume. The bulk density was then calculated by dividing the mass of the powder by the bulk volume. The tapped density was determined by tapping the measuring cylinder manually on a flat surface for 3 min until no further change in powder volume was observed. The final volume was recorded as the tapped volume. The tapped density was then calculated by dividing the mass of the powder by the tapped volume. The flowability and cohesiveness of the powder were assessed using the Hausner ratio (HR) (Hausner, 1967) and Carr's index (Carr, 1965) respectively, and calculated as follows:

$$HR = \frac{\rho_{tapped}}{\rho_{bulk}} \quad (3)$$

$$Carr's\ Index = \left(\frac{\rho_{tapped} - \rho_{bulk}}{\rho_{tapped}}\right) \times 100 \quad (4)$$

Where ρ_{bulk} is the bulk density and ρ_{tapped} is the tapped density. In general, a lower Hausner ratio and Carr's index indicate better flow characteristics. The classification of flowability based on HR and Carr's Index values is presented in Table 2.

2.5.4. Bulk compression test

Bulk compression tests were performed following the method of Farshchi et al. (2022) with minor modifications. Measurements were conducted using a texture analyzer (Brookfield CT3 Texture Analyzer, Middleboro, MA, USA) equipped with a 50 kg load cell (≈490 N), which had a resolution of 5.0 g. A pre-weighed mass of the beetroot powders was poured into an acrylic cylindrical cup (inner diameter of 25.6 mm, height 30 mm) through a glass funnel and tapped until the volume did not decrease any further. The powders were then compressed with a close-fitting probe (TA11, 25.4 mm) under a normal force of 40 kg. The compression behavior and the compaction mechanism of the beetroot powders were analyzed using the Kawakita model. This empirical equation was proposed by Kawakita and Lüdde (1971) for analysis of soft and fluffy powders, which expresses the relationship between volume and applied pressure during compression, Eq. (5).

$$\frac{P}{C} = \frac{1}{ab} + \frac{P}{a} \quad (5)$$

Here, C represents the degree of volume reduction, calculated as $C = (V_0 - V)/V_0$, where V_0 is the initial bulk volume and V is the volume under compression at pressure P. The constants a and b are known as the Kawakita parameters. The parameter a reflects the maximum compressibility and is often associated with initial bed porosity, representing the extent of compression at infinite pressure. In contrast, b relates to the material's resistance to compression, with $1/b$ corresponding to the pressure needed to reach half of the maximum volume reduction ($a/2$). Previous studies (Khomane et al., 2013) have linked $1/b$ to yield strength and the plastic deformation behavior of powders. The Kawakita parameters were extracted from the slope and intercept of the linear plot of P/C versus P, obtained via regression analysis.

2.5.5. Tablet strength measurement

For the tablet preparation, 1.0 g of freeze-dried beetroot powders was carefully poured into an acrylic cylindrical split die with a diameter of 25.6 mm (Fig. 1) using a glass funnel and tapped manually on a flat surface for 3 min. The beetroot powders were compressed under a normal force of 40 kg. The tablets were then removed from the die and analyzed using a texture analyzer (Brookfield CT3 Texture Analyzer, Middleboro, MA, USA) equipped with a 4.5 kg load cell (≈44 N), which had a resolution of 0.5 g. The uniaxial tensile strength was measured by the diametral-compression test, applying a constant speed of 0.1 mm/s. For this purpose, the tablets were placed on their sides and crushed along their vertical axis. The force-displacement curves obtained from the compression tests were then analyzed to calculate the tablet tensile strength, σ_t, using the following equation (Ong et al., 2014).

$$\sigma_t = \frac{2F_r}{\pi dy} \quad (6)$$

Where F_r is the rupture force, d is the tablet diameter, and y is the tablet thickness. The rupture force was determined manually from the peak failure point in the force-displacement curves, typically identified as the first sharp drop in the applied force (Fig. 1).

Table 2
Classification of powder flowability based on HR and Carr's Index (Lebrun et al., 2012).

Flow Behavior	Hausner ratio	Carr's index (%)
Excellent Flow	1.00–1.11	<10
Good/Free Flow	1.12–1.18	11–15
Fair	1.19–1.25	16–20
Passable	1.26–1.34	21–25
Poor Flow/Cohesive	1.35–1.45	26–31
Very Poor Flow/Very Cohesive	1.46–1.59	32–37
Extremely Poor Flow	>1.60	>38

2.5.6. Color measurements

Color parameters of the beetroot powders were determined using a hand-held spectrocolorimeter (Lovibond® LC100, China) employing the CIE D65 illuminant and a 10° observation angle. The color measurements were expressed in terms of L*, a*, b*, C*, and h°. The L* parameter represents lightness, ranging from 0 (black) to 100 (white). The a* value indicates the red to green spectrum, with positive values representing redness and negative values indicating greenness. The b* value represents the blue to yellow spectrum, with positive values indicating yellowness and negative values indicating blueness. The hue angle (h°) represents the type of color perceived by the human eye and is expressed in degrees, with 0°, 90°, 180°, and 270° corresponding to red, yellow, green, and blue, respectively. The chroma (C*) represents the saturation or intensity of the color.

The hue angle (h°), chroma (C*), and total color difference (ΔE) were calculated using the following equations (Aghajanzadeh et al., 2023):

$$Hue\ angle\ (h^\circ) = \tan^{-1}\frac{b^*}{a^*} \quad (7)$$

$$C^* = \sqrt{(a^*)^2 + (b^*)^2} \quad (8)$$

$$\Delta E = \sqrt{(\Delta L^*)^2 + (\Delta a^*)^2 + (\Delta b^*)^2} \quad (9)$$

where ΔL*, Δa*, and Δb* represent the differences in color parameters between the beetroot tablets and a white standard plate.

3. Results and discussions

3.1. Foam properties

3.1.1. Foam capacity and foam density

The incorporation of air bubbles into liquids modifies food texture, leading to a more semi-solid behavior, and altering the mouthfeel and appearance of the food (Sadahira et al., 2018). Foam expansion, which measures the amount of air incorporated into the foam, and foam density of the samples are shown in Fig. 2. The addition of maltodextrin to formulations containing egg white protein, slightly enhanced foam expansion, reaching approximately 460 % compared to ~450 % for the control (EP). This slight improvement can be attributed to the increased viscosity of the continuous phase, resulting from properties of maltodextrin as a polysaccharide thickening agent. The increased viscosity helps reduce the likelihood of bubble coarsening, which may occur immediately after the whipping process, followed by the possible loss of such large bubbles. This observation is consistent with the study by Sun et al. (2022), who demonstrated that the addition of saccharides, particularly maltodextrin, significantly improved the foaming properties of egg white solutions. This was attributed to increased apparent viscosity, enhanced surface hydrophobicity, and reduced surface tension at higher saccharide concentrations. These physicochemical changes were associated with improved foam capacity and stability. However, as noted by Chandrakar et al. (2024), this synergistic effect is concentration-dependent. The authors reported that while moderate levels of maltodextrin enhance foam expansion due to increased viscosity, excessive viscosity may hinder the rapid diffusion of protein

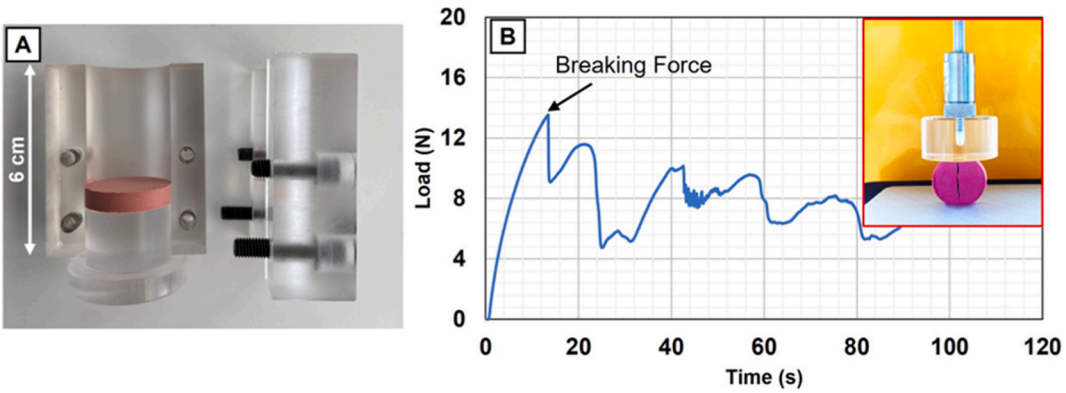

Fig. 1. (A) Split acrylic compaction die used for tablet formation. (B) A typical force-displacement curve obtained from the texture analyzer during the diametral compression test of a beetroot tablet. The first sharp peak corresponds to the breaking force, as indicated on the graph. The inset shows an image of a beetroot tablet breaking at the moment of rupture, captured during the compression test.

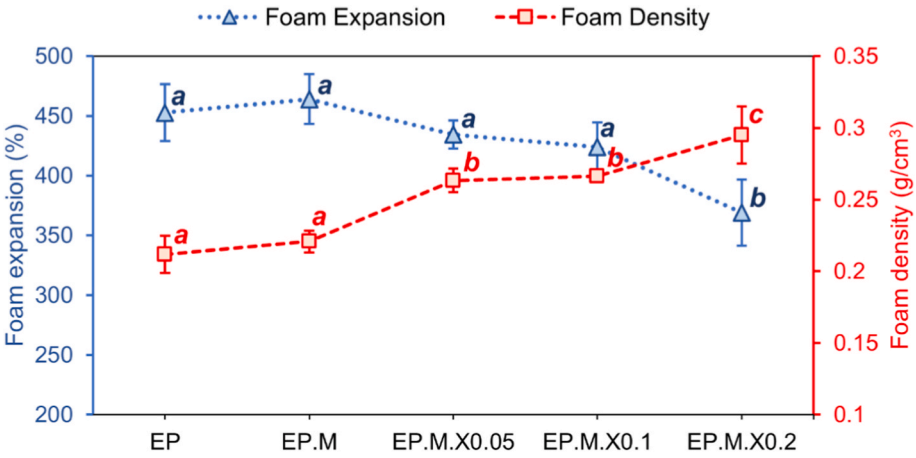

Fig. 2. Foam expansion (%) and foam density (g/cm^3) of beetroot juice foams prepared with different stabilizers. Bars represent ± standard deviation (SD, n = 4). Different letters above the bars indicate significant differences among formulations ($p < 0.05$, Tukey's honestly significant difference (HSD) test).

molecules at the gas-liquid interface and the formation of a stable film, thus weakening the protein foam capacity (Raikos et al., 2007). This dual effect became evident with the addition of xanthan gum to the EP.M formulations. Foam expansion decreased to 430 % for EP.M.X0.05 and progressively declined with higher concentrations of xanthan gum. In contrast, the foam density increased from 0.22 g/cm^3 in the EP.M samples to 0.26 g/cm^3 in EP.M.X0.05, and reached the highest value of 0.29 g/cm^3 for EP.M.X0.2. The slightly higher foam density observed in the EP.M sample compared to EP, despite its greater foam expansion, may be attributed to the increased liquid density introduced by maltodextrin. The overall trend reflects a shift in the foam's structural balance as thickening agents were added.

These findings align closely with the results reported by Dabestani and Yeganehzad (2019), who observed similar trends in their studies involving egg white protein-based foams supplemented with xanthan gum. The authors reported increases in foam density and corresponding decreases in overrun as xanthan gum concentration was raised. They concluded that the decreased overrun results from xanthan gum enhancing the viscous properties of the mixture, which inhibits excessive air incorporation and improves the retention of the liquid phase within the foam structure. Indeed, the higher molecular weight of xanthan gum, coupled with its capability to form extensive networks of entangled chains, establishes it as a hydrocolloid with a superior ability to enhance bulk viscosity at relatively low concentrations compared to maltodextrin (Nsengiyumva and Alexandridis, 2022).

3.1.2. *Foam firmness*

Foam firmness is a key physical property largely determined by the aeration process, which in turn is influenced by factors such as the level of aeration and the distribution of bubble sizes. The firmness and fracture properties of the matrix in which the bubbles are embedded are critical as they affect the foam's rheology, its breakdown during consumption, and even flavor release (Minor et al., 2009). Therefore, understanding foam firmness is essential for optimizing foam structure for the desired mouthfeel and overall consumer acceptance. Fig. 3 illustrates the firmness of foam samples measured by a texture analyzer as

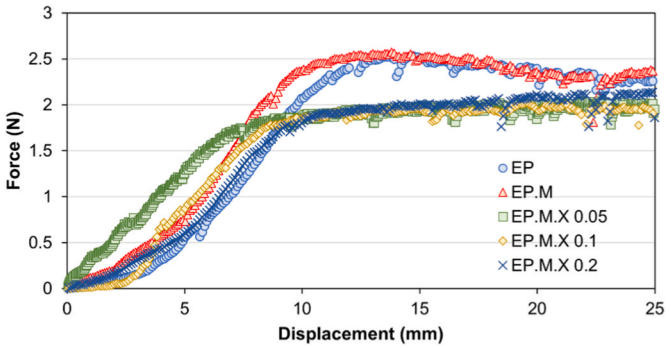

Fig. 3. Force-displacement curves representing the firmness of beetroot foams with different stabilizer formulations.

described in section 2.4.3. Among all samples, the EP.M formulation showed the highest foam firmness (~2.60 N), followed closely by the control sample (EP), which showed a slightly lower firmness (~2.53 N). However, the addition of xanthan gum at 0.05 wt% led to a noticeable reduction in firmness to approximately 2.04 N. Increasing the concentration to 0.1 wt% (EP.M.X0.1) continued this downward trend, lowering the firmness to approximately 2.02 N. The results are aligned with the findings of Nooshkam et al. (2022), who reported that protein-polysaccharide foams with the highest overrun and lowest density showed the highest firmness value, which can be attributed to the formation of a more closely packed, touching bubble structure within the foam, thereby enhancing its solid-like characteristics (Yang and Foegeding, 2011). Yang and Foegeding (2011) investigated foam yield stress, as a measure of the structural strength, and interfacial properties of foams made from mixtures of egg white protein and sucrose. They found that increase in viscosity led to a lower foam yield stress, mainly due to the reduced air phase fraction.

Interestingly, the addition of 0.2 wt% xanthan to beetroot juice samples resulted in a slightly higher firmness (2.13 N) compared to those containing lower xanthan concentrations. While lower concentrations primarily influence foam textures by increasing the viscosity of the continuous phase and reducing the air fraction, the further addition of xanthan to 0.2 wt% may have altered the bulk phase to exhibit more viscoelastic properties. The increased firmness can be attributed to the formation of a three-dimensional network of entanglement polymer, leading to gel-like characteristics. This viscoelastic-concentration dependence of xanthan gum above a critical concentration in solutions has been previously demonstrated by Wyatt and Liberatore (2009).

3.1.3. Foam stability

The role of xanthan gum and maltodextrin as thickening agents and viscosity enhancers in the continuous aqueous phase is further illustrated in Fig. 4, which shows foam stability based on drainage volume over time. This visualization highlights the impact of these additives on maintaining foam structure and reducing liquid loss. Since foams are thermodynamically unstable systems, enhancing their kinetic stability is crucial prior to foam-mat drying processes. During drying, moisture migration is driven by capillary action within the structure of the foam. Therefore, improving foam stability is essential for efficient moisture removal, leading to quicker drying processes, easier removal of dried materials from trays, and improved quality of the final product (Maciel et al., 2022). In this study, the addition of polysaccharides made the greatest contribution for this purpose. The sample containing only egg white protein (EP) demonstrated immediate and notable drainage, with 10 mL of liquid separating within the first few minutes after the whipping process, indicating poor initial stability. This rapid separation suggests that the foam structure was unable to retain liquid effectively in its early stages. Over time, drainage continued gradually, plateauing at approximately 70 mL after around 100 min. The sample that included

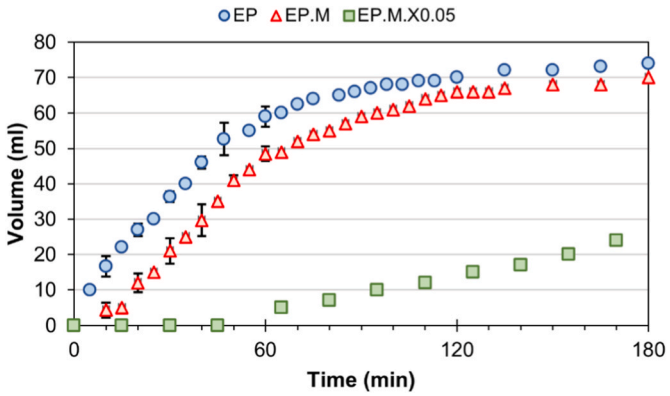

Fig. 4. Drainage volume of foams over time, for different sample formulations.

the addition of maltodextrin (EP.M) demonstrated enhanced initial stability, showing no drainage in the first 5 min. This suggests that maltodextrin enhances the viscosity of the liquid phase, effectively retaining the liquid within the foam structure during the initial stages. Although the sample followed a similar overall trend to EP, the EP.M achieved a slightly lower drainage volume at a slower rate throughout the 180-min period. The formulation containing both maltodextrin and 0.05 wt% xanthan gum (EP.M.X0.05) demonstrated even greater stability, with no drainage at all in the first 60 min and a significantly lower final drainage volume (less than 40 mL) at the end of the 180-min period. This significant reduction in the drainage volume compared to the other samples further highlights xanthan gum's role as a potent thickening agent, enhancing the foam's structural integrity by effectively reducing the rate and total volume of drainage. Interestingly, the samples with higher concentrations of xanthan gum (0.1 and 0.2 wt%) exhibited no drainage over the entire measurement period, underscoring the powerful stabilizing effect of xanthan gum at these increased concentrations.

The influence of xanthan gum as a thickening agent on foam stability can be further elucidated through microscopic observations of beetroot juice foam samples (EP, EP.M, and EP.M.X0.05), captured at two different times: 15 min and 45 min, post-whipping. The micrographs are shown in Fig. 5. After 15 min of whipping, all samples displayed spherical bubbles dispersed in a liquid phase, with the EP and EP.M samples exhibiting a larger number of bubbles. In contrast, the EP.M.X0.05 samples show fewer, more uniformly distributed bubbles with a noticeably thicker liquid phase between them. This aligns with our expectations, where, as discussed previously, the presence of xanthan gum in the EP.M.X0.05 samples leads to a higher foam density and a reduced rate of foam expansion.

After 45 min post-whipping, the distinction between samples becomes even more pronounced. This is especially the case in the EP and EP.M samples that do not contain xanthan gum. In these samples, bubbles begin to lose their perfect spherical character, transitioning toward polyhedral shapes. This visual change is attributed primarily to liquid drainage and bubble creaming, which increase the relative air volume fraction in the foam and reduce the liquid content between bubbles. As a result, bubbles become more closely packed at the top, promoting more rigid packing geometries. (Murray, 2007; Xu et al., 2020). In contrast, the EP.M.X0.05 samples retain their initial spherical form, though they are larger in size and are not as closely packed.

3.2. Powder properties

3.2.1. Moisture sorption properties and solubility index

Fig. 6 illustrates the moisture sorption properties of various beetroot powder formulations, as obtained through Dynamic Vapor Sorption (DVS) measurements. The base formulation, containing only 5.0 wt% egg white protein (EP), exhibits a typical sorption pattern of sugar-rich foods (Al-Muhtaseb et al., 2002). This pattern is characterized by a slow linear increase in sorption at low humidities (RH<30 %), which becomes progressively steeper at intermediate humidities (30–60 % RH), culminating in a sharp rise above 60 % RH. The noticeable increase in equilibrium moisture content (EMC) values above 50 % RH indicates a shift in the water sorption mechanism. Various mechanisms have been identified to explain how water vapor interacts with adsorbent molecules, including surface adsorption, bulk adsorption, hydration, gelation, and deliquescence (Ouyang et al., 2015). At lower relative humidity levels, water vapor sorption is driven by entropy, related to the availability of sorption sites and the randomness of water molecule movement. As relative humidity increases, more polar sites become occupied, enhancing the systematic organization within the system and leading to the formation of additional adsorbate layers (Bonilla et al., 2010). Consequently, the relatively modest moisture uptake observed up to 50 % RH is primarily due to surface adsorption, influenced by the micro-structure of the powder. Conversely, at medium to high humidity

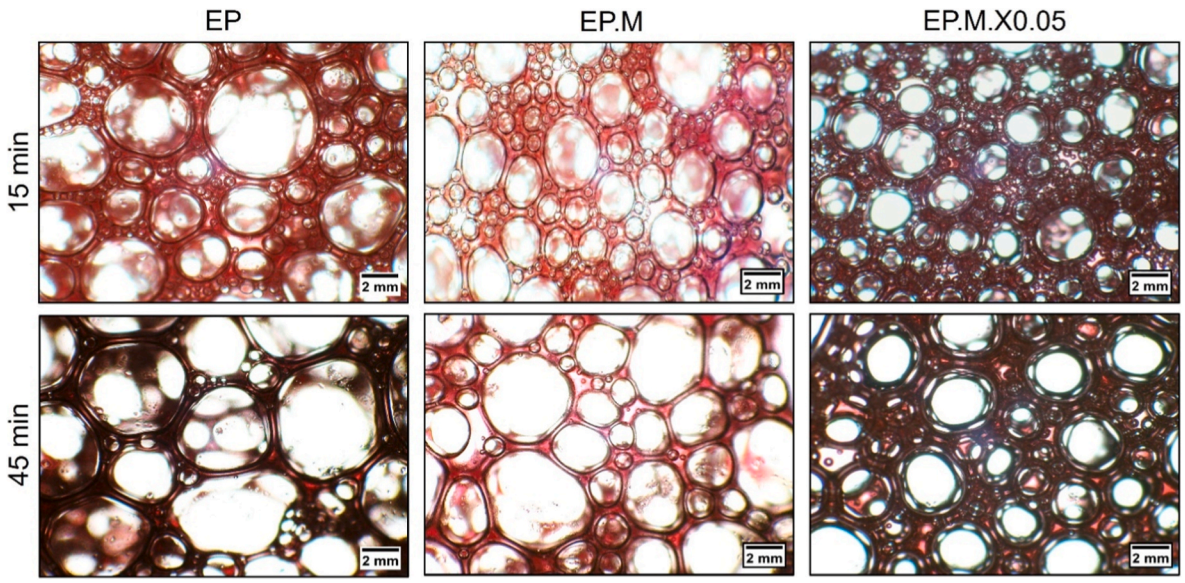

Fig. 5. Microscopic images of beetroot juice foams after 15 min (top) and 45 min (bottom) post-whipping, showing the influence of the addition of the thickening agent on foam stability and bubble morphology.

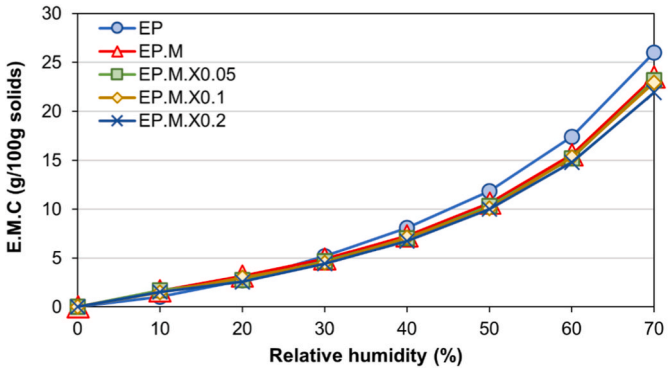

Fig. 6. Equilibrium moisture content (E.M.C, g/100 g solids) of foam-mat freeze-dried beetroot powders as a function of relative humidity at 25 °C.

levels, bulk water sorption becomes the predominant process. This phase often involves significant interactions between the sorbate and the sorbent, resulting in structural changes such as dissolution, swelling, and glass transition. Therefore, a remarkable moisture uptake above 50 % RH can be attributed to dominant solute–solvent interactions associated with sugar dissolution (Mosquera et al., 2012; Ozcelik et al., 2020).

The addition of maltodextrin (EP.M) significantly altered the sorption curve above 40 % RH, although the overall moisture uptake remained similar to that of EP alone. The subsequent additions of xanthan gum at concentrations of 0.05 wt% and 0.1 wt% (EP.M.X0.05 and EP.M.X0.1) did not show a noticeable difference from EP.M in terms of moisture uptake. However, the equilibrium moisture content (EMC) was slightly reduced with the addition of 0.2 wt% xanthan gum (EP.M.X0.2) at 70 % RH. The noticeable decreases in the hygroscopic properties of the powders, from 26.01 % in control samples (EP) to 23.49 % with the addition of maltodextrin, and further to 21.92 % with the highest rate of xanthan gum addition, can be attributed to the higher molecular weight of these polymers compared to the naturally occurring sugar compounds in beetroot extract. The larger molecular size of maltodextrin and xanthan gum leads to a lower affinity for moisture sorption (Bhusari et al., 2014). This is because these polymers interact differently with water molecules compared to smaller sugar molecules, which typically form more readily reversible bonds with water. The structure and composition of these biopolymers reduce the number of active sites available for water binding, consequently decreasing the overall hygroscopicity of the resulting beetroot powders (Carmo et al., 2018).

The influence of the molecular weight of xanthan is further reflected in the solubility index measurements of the beetroot powder formulations (Table 3). The control samples, containing only 5.0 wt% egg white protein, demonstrated the highest solubility at 92.05 ± 0.98 %. The inclusion of maltodextrin (EP.M) resulted in a slight reduction in solubility (91.70 ± 1.34 %), but this difference was not significant, as both values fall within overlapping margins of error. However, the addition of xanthan gum adversely affected the solubility of reconstituted beetroot powders. As the concentration of xanthan gum increased, a more pronounced decrease in solubility was observed, with the lowest solubility reaching 77.27 ± 0.67 % at the highest xanthan concentration.

This reduction is likely attributed to the higher molecular weight and gelling behavior of xanthan gum, which increases solution viscosity and slows the hydration and dispersion of powder particles during reconstitution (Ren et al., 2024).

3.2.2. *Powder morphology and flowability*

The flowability of powders, a critical property in the manufacturing of solid dosage forms such as tablets, was assessed using two established metrics: the Hausner Ratio (HR) and Carr's Index (CI). The HR is widely used as an indicator of powder flowability, with lower values reflecting better flow characteristics. In contrast, Carr's Index measures powder cohesiveness and compressibility, with higher values indicating greater cohesiveness and poorer flow performance.

The results (Table 3) show that the powder containing only egg white protein (EP) exhibited an HR of 1.32 and a Carr's Index of 24.44 %, classifying it within the passable flow range. The addition of maltodextrin (EP.M) slightly improved flowability, reducing the HR to 1.29 and CI to 22.52 %, thus maintaining a passable classification while indicating marginally lower cohesiveness compared to EP. Upon incorporating xanthan gum, a progressive deterioration in flowability and a corresponding increase in cohesiveness were observed with increasing concentration. The formulation containing 0.05 wt% xanthan gum (EP.M.X0.05) remained within the passable range but exhibited slightly reduced flow compared to EP.M. However, as xanthan concentration increased to 0.1 wt% and 0.2 wt%, the powders approached and eventually crossed the threshold into poor flow behavior, as indicated by markedly higher HR and CI values.

Table 3
Powder density, flowability indices, hygroscopicity, and solubility of foam-mat freeze-dried beetroot powders containing different carrier formulations.

Sample	Loose Density (g/cm^3)	Tapped Density (g/cm^3)	Hausner Ratio (HR)	Carr's Index (%)	EMC at 70 % RH (g H_2O/100 g solids)	Solubility (%)
EP	0.33	0.44	1.32 ± 0.00^a	24.44 ± 0.00^a	26.01	92.05 ± 0.98^a
EP.M	0.33	0.43	1.29 ± 0.01^a	22.52 ± 0.43^a	23.49	91.70 ± 1.34^a
EP.M.X0.05	0.32	0.43	1.33 ± 0.02^a	24.59 ± 0.95^a	23.16	88.85 ± 0.71^b
EP.M.X0.1	0.31	0.42	1.35 ± 0.02^a	25.90 ± 0.90^a	22.94	86.47 ± 0.74^b
EP.M.X0.2	0.29	0.42	1.47 ± 0.01^b	31.90 ± 0.67^b	21.92	77.27 ± 0.67^c

*Different superscript letters within the same column indicate significant differences among formulations ($p < 0.05$, Tukey's honestly significant difference (HSD) test).

The improvement in flowability observed with maltodextrin aligns with previous studies. Carrier agents such as maltodextrin are known to enhance powder flow in sugar-containing systems, primarily through increasing the glass transition temperature (*Tg*) and thereby reducing hygroscopicity and moisture absorption—two critical contributors to powder cohesiveness (Kalajahi et al., 2023). In the present study, the EP.M formulation demonstrated the best flow behavior, which supports this mechanism. For example, Islam et al. (2024) reported that microwave-assisted foam-mat dried jackfruit juice powders produced at higher maltodextrin-to-egg white protein ratios exhibited lower moisture content and improved flowability, attributed to the reduced hygroscopicity from maltodextrin. Similarly, Hajiaghaei and Sharifi (2022) found that increasing maltodextrin concentration up to 20 % in foam-mat freeze-dried red beetroot formulations improved flow properties, resulting in the lowest HR and CI values. However, in the present study, the powders were equilibrated at 11 % relative humidity (RH) for one week prior to density measurements, and sorption isotherm data (Fig. 6) confirmed that equilibrium moisture content was similar across samples at this RH level. Moisture uptake remained minimal up to 30 % RH, suggesting that differences in hygroscopicity were not the primary cause of the observed flowability differences. This points to other physicochemical factors—particularly particle size and morphology—as likely contributors.

In foam-mat drying, foam density and expansion critically influence the structure of the resulting dried material. Lower-density, high-expansion foams tend to form thinner lamellae that break into finer, more fragmented particles during grinding, while denser foams form thicker lamellae that result in larger, bulkier particles (Mounir, 2017). In the current study, the addition of xanthan gum led to foams with higher density and reduced expansion, which likely resulted in the formation of thicker lamellae and, consequently, the larger, irregular particles observed in SEM and light microscopy images. These morphological observations help explain the poor flow properties observed in xanthan-containing powders. SEM images revealed that, while all samples exhibited rough and fragmented surfaces, the formulations with 0.1 and 0.2 wt% xanthan (Fig. 7C and D) displayed prominent large, irregular granules interspersed with smaller fragments. This heterogeneity in particle size and shape likely disrupted efficient particle packing and promoted mechanical interlocking—both factors that contribute to increased cohesiveness and reduced bulk density (Kulkarni et al., 2023). This was also quantitatively reflected in the measured loose bulk density values, which declined progressively from 0.33 g/cm^3 in EP and EP.M to 0.29 g/cm^3 in EP.M.X0.2 (Table 3). The lower bulk densities observed in xanthan-containing formulations support the conclusion that their

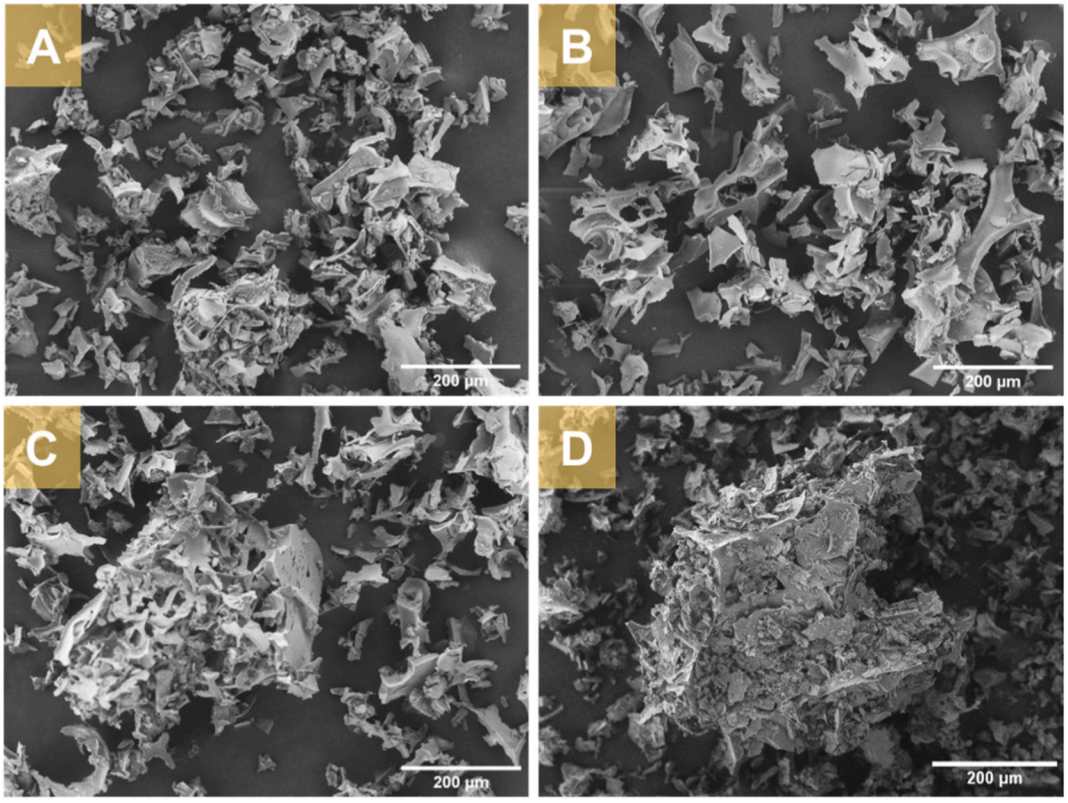

Fig. 7. Scanning electron micrographs of freeze-dried beetroot powders: (A) EP (egg white protein only), (B) EP.M (egg white protein + maltodextrin), (C) EP.M.X0.1 (egg white protein + maltodextrin +0.1 wt% xanthan gum), and (D) EP.M.X0.2 (egg white protein + maltodextrin +0.2 wt% xanthan gum).

particle morphology contributed to looser packing and poorer flowability. Overall, these findings demonstrate that the addition of carrier agents such as foam stabilizers plays a key role in defining foam microstructure, which in turn leads to powders with distinct morphologies after grinding and consequently different powder flow properties.

3.2.3. Compressibility analysis

The compressibility behavior of beetroot powder formulations was evaluated through strain–pressure curves (Fig. 8a) and Kawakita profiles (Fig. 8b). The Kawakita constant a represents the maximum achievable compressibility, reflecting the powder bed's capacity for volume reduction, while the parameter *1/b* indicates the pressure required to achieve half of this maximum compressibility (*a/2*), commonly associated with the internal cohesion or interparticle friction of the powder bed (Fig. 8c and d).

The EP formulation showed a gradual and sustained increase in strain with compression pressure (Fig. 8a), suggesting a slower but progressive deformation of the powder bed. This profile aligns with its relatively high *a* value (Fig. 8c), indicating a greater overall degree of compressibility at infinite pressure. Although the Kawakita constant *a* is often associated with initial porosity, bulk density measurements (Table 3) showed that EP had the highest loose and tapped densities, suggesting a relatively compact initial bed. Therefore, the elevated *a* value is more likely attributed to the plastic deformation behavior of the powders under pressure, allowing for significant volume reduction despite the relatively compact initial bed. This interpretation aligns with previous studies, where the Kawakita parameter *a* was closely linked to the maximal engineering strain, serving as an effective indicator of the plastic deformation capacity of granular solids under applied compression pressure (Nordström et al., 2008). Furthermore, the high *1/b* value observed for EP (Fig. 8d) supports significant internal cohesion and greater resistance to compaction, likely arising from pronounced frictional plastic deformation and mechanical interlocking at particle contacts.

The incorporation of maltodextrin into the EP matrix (EP.M) significantly altered the compression behavior. The EP.M sample demonstrated a sharp increase in strain at low pressures, followed by a more gradual rise (Fig. 8a), suggesting quicker particle rearrangement and early-stage consolidation. This is consistent with its improved flowability, as evidenced by lower Hausner Ratio and Carr's Index values. The reduction in the *a* value (Fig. 8c) indicates a decrease in total compressibility, likely reflecting the stiffening effect introduced by maltodextrin. Additionally, the reduced *1/b* value (Fig. 8d) in EP.M compared to EP suggests a lower resistance to compression, indicating improved particle rearrangement in the initial stages of compression, consistent with the sharper strain increase observed at low pressures (Fig. 8a)

Upon addition of 0.05 wt% xanthan gum (EP.M.X0.05), the *a* value further decreased, suggesting reduced compressibility, while the *1/b* value increased again, indicating increased internal friction or resistance during compression. This is supported by SEM micrographs (Fig. 7C–D), which show the formation of larger, more irregularly shaped granules with rougher surfaces in xanthan-containing powders. These features are likely to restrict powder particle rearrangements and enhance frictional resistance during compression, resulting in a higher level of internal cohesion. At higher xanthan concentrations (0.1 and 0.2 wt%), no significant changes were observed in either *a* or *1/b* values, as they remained within the margin of error.

3.3. Tablet properties

The measured tablet thickness and density closely align with the compressibility behavior captured by the Kawakita parameter (Table 4). The EP formulation exhibited the smallest thickness and highest density (0.60 cm, 0.65 g/cm^3), consistent with its highest *a* value, indicating significant volume reduction and compressibility under pressure. Upon incorporating maltodextrin (EP.M), tablet thickness slightly increased and density decreased, demonstrating reduced compressibility and powder-bed compactness. This trend continued with increasing xanthan gum contents (EP.M.X0.05 to 0.2), where tablet thickness progressively increased and density decreased, in agreement with declining *a* values across these formulations.

Tensile strength measurements further highlighted the influence of compressibility behavior and structural composition. A significant decrease in tensile strength was observed between EP and EP.M tablets, correlating with increased tablet thickness and reduced compactness.

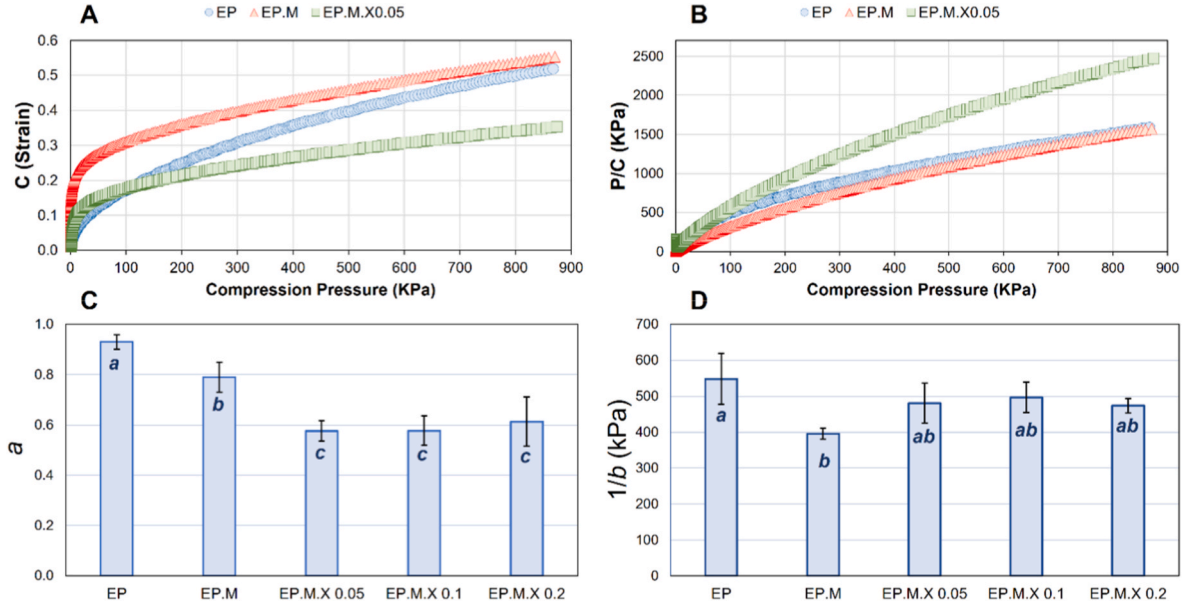

Fig. 8. Compressibility analysis of freeze-dried beetroot powders using the Kawakita model. (A) Strain–pressure curves and (B) Kawakita plots (*P/C* vs. *P*) show typical profiles for selected samples (EP, EP.M, and EP.M.X 0.05). (C) Kawakita constant *a* and (D) *1/b* values are presented for all formulations. Bars represent ± SD (n = 3). Different letters below the bars indicate significant differences among formulations ($p < 0.05$, Tukey's HSD test); formulations labelled by a common letter are not significantly different to each other.

Table 4
Color and physical properties (thickness, density, and tensile strength) of beetroot tablets.

Tablet	Color parameters (Lovibond® Spectrocolorimeter)						Thickness (cm)	Density (g/cm^3)	Tensile strength (N/cm^2)
	L*	a*	b*	c*	$\overset{\circ}{h}$	ΔE			
EP	43.20 ± 1.69^{a}	38.70 ± 1.69^{a}	10.70 ± 3.82^{a}	40.20 ± 2.68^{a}	15.30 ± 4.67^{a}	69.65 ± 2.89^{a}	0.60 ± 0.00^{a}	0.65 ± 0.00^{a}	0.42 ± 0.01^{a}
EP.M	50.45 ± 0.07^{b}	37.15 ± 0.35^{a}	5.55 ± 0.77^{ab}	37.60 ± 0.42^{b}	8.45 ± 1.06^{b}	62.2 ± 0.28^{b}	0.63 ± 0.02^{a}	0.61 ± 0.02^{a}	0.31 ± 0.05^{b}
EP.M. X0.05	52.90 ± 0.84^{bc}	34.50 ± 0.56^{b}	8.65 ± 3.46^{b}	35.60 ± 1.41^{b}	13.95 ± 5.16^{a}	59.05 ± 1.48^{bc}	0.67 ± 0.03^{b}	0.58 ± 0.03^{b}	0.38 ± 0.01^{a}
EP.M. X0.1	53.90 ± 0.28^{c}	35.10 ± 0.28^{b}	5.35 ± 0.07^{b}	35.50 ± 0.28^{b}	8.65 ± 0.07^{b}	58.15 ± 0.35^{bc}	0.72 ± 0.03^{b}	0.54 ± 0.02^{b}	0.37 ± 0.01^{a}
EP.M. X0.2	55.45 ± 0.77^{d}	34.10 ± 0.13^{b}	4.65 ± 0.35^{b}	34.40 ± 1.13^{b}	7.90 ± 0.14^{b}	56.30 ± 1.27^{c}	0.80 ± 0.00^{c}	0.49 ± 0.00^{c}	0.38 ± 0.04^{a}

* Values represent ± standard deviation (SD, n = 3–4). Means within the same column followed by different superscript letters differ significantly ($p < 0.05$, Tukey's HSD test).

This reduction may be attributed, firstly, to the dilution effect introduced by the addition of maltodextrin as a carrier agent, which reduced the proportion of beetroot solids that inherently possessed stronger interparticle bonding properties (Al-Ibraheemi et al., 2013). Such dilution inherently weakened the mechanical strength and cohesion of the original beetroot powder matrix. Secondly, the addition of maltodextrin introduced materials with distinct deformation characteristics compared to native beetroot powders. Amin and Fell (2004) suggested that mixing powders with differing mechanical behaviors (plastic and brittle) can disrupt interparticle bonding and create percolation thresholds, leading to abrupt changes in mechanical properties. This phenomenon likely contributed to the observed decline in tensile strength with maltodextrin incorporation.

The trend of increasing thickness and decreasing density became more pronounced with the progressive addition of xanthan gum. As earlier shown in Fig. 7, scanning electron microscopy (SEM) observations indicated the presence of larger and more irregular particles in xanthan-containing samples, which likely contributed to less efficient packing and increased porosity.

From a material perspective, low-molecular-weight compounds, such as sugars present in beetroot powders, typically exhibit greater plastic deformation, facilitating stronger and more permanent interparticle bonds during compression. In contrast, high-molecular-weight biopolymers like xanthan and maltodextrin tend to deform more elastically under pressure (Steendam et al., 2001). This inherent viscoelastic behavior of the added biopolymers is expected to compromise the formation of robust interparticle bonds, contributing to the overall reduction in mechanical integrity of the tablets.

However, despite continued reductions in tablet density with increasing xanthan gum content, a modest recovery in tensile strength, compared with the EP.M samples, was observed across formulations EP.M.X 0.05 to 0.2. This improvement suggests that xanthan gum may promote localized structural reinforcement, potentially through mechanical interlocking among irregularly shaped particles or viscoelastic bridging effects, partially offsetting the compromised bonding caused by earlier maltodextrin addition. Morphological evidence from SEM analysis (Fig. 7C–D) further supports this interpretation, showing that xanthan-containing samples exhibited denser, irregular particles that contrasted with the finer and more fragmented structure of the maltodextrin-based powder. This observation aligns with the increase in the Kawakita *1/b* value (Fig. 8D), indicating increased internal friction and resistance to densification compared to EP.M.

Color is an important quality attribute of compressed vegetable powders, particularly when used as nutritional colorants (Mehrali et al., 2025). In this study, the color properties of the tablets, particularly L* (lightness) and a* (redness), were noticeably influenced by the addition of maltodextrin and xanthan gum (Table 4). Incorporation of maltodextrin into the formulation (EP.M) resulted in an increase in L* values and a decrease in a* values, indicating a lighter and less red appearance of the tablets. This shift can primarily be attributed to the intrinsic whiteness of maltodextrin, which diluted the concentration of beetroot pigments responsible for the intense red color. Similar observations have been reported in beetroot powders by Ng and Sulaiman (2018) and García-Segovia et al. (2021), where the addition of carrier agents led to brighter and less intensely colored powders.

In xanthan-containing tablets (EP.M.X 0.05 to 0.2), a further increase in L* and a decrease in a* values were observed compared to the maltodextrin-only sample (EP.M), although differences among xanthan concentrations were not significant. The overall increase in lightness observed in the xanthan-containing formulations can be attributed to the combined effect of the added carrier material and the reduced compactness of the tablets, resulting in a lower solid fraction and a dilution of the apparent color intensity (Siddiqui and Nazzal, 2007). Overall, the tablet results show that carrier agents strongly influenced both mechanical strength and appearance. Maltodextrin reduced compactness and tensile strength, mainly due to dilution effects and altered deformation behaviour, while xanthan gum partly restored strength through mechanical interlocking among more irregularly shaped particles. These outcomes are consistent with the observations reported earlier in this study on powder morphology and compressibility, highlighting the process–structure–property relationship from foam stabilization to tablet formation. The carrier agents not only affected structural integrity but also modified tablet appearance through both the dilution of beetroot pigments and the reduced compactness of the tablets.

4. Conclusion

This study demonstrated the use of foam-mat freeze-drying to produce functional beetroot powders and highlighted the distinct roles of maltodextrin and xanthan gum in shaping physicochemical and compressibility properties. It was shown that maltodextrin enhanced foam expansion, reduced hygroscopicity, and improved flowability, whereas xanthan gum significantly increased foam stability and reduced drainage, but led to powders with more irregularly shaped particles, reduced solubility, and poor flow characteristics at the highest examined concentration. Integrated evidence from foam characterization, optical microscopy, and SEM established a clear structure–property link: xanthan-containing foams (particularly at higher levels) showed increased density and reduced expansion with thicker lamellae, which translated, after freeze-drying and subsequent grinding, into a heterogeneous mixture of coarser and finer particles. This morphology likely promoted higher internal friction and localized mechanical interlocking, explaining the partial recovery of tablet strength and increased resistance to densification during compression. Tablet characterization further revealed that carrier addition altered compressibility behavior and tensile strength, with xanthan contributing to modest strength recovery through structural interlocking. Color measurements showed that both carriers diluted pigment concentration, resulting in lighter-colored tablets.

Building on these findings, future work can extend the current physicochemical and mechanical characterization toward in-use

performance and consumer perception. In particular, it would be valuable to study tablet disintegration kinetics and reconstitution behavior under realistic preparation conditions (e.g. different liquid media, temperatures and mixing conditions), and to systematically assess sensory attributes such as mouthfeel, perceived chalkiness, flavor release and overall acceptability of the resulting tablets and reconstituted drinks. Coupling such sensory and consumer data with the structure–property relationships established in this work would provide product development scientists with a stronger basis for designing beetroot-based nutraceutical tablets and plant-based food supplements with targeted functional and sensory profiles.

CRediT authorship contribution statement

Vamsi Pavan Kumar Boddapati: Writing – original draft, Methodology, Investigation. **Sareena Vanchipurackal Sherif:** Investigation. **Jabbar Gardy:** Investigation. **Ali Hassnapour:** Writing – review & editing. **Rammile Ettelaie:** Writing – review & editing. **Amin Farshchi:** Writing – review & editing, Supervision, Project administration, Methodology, Formal analysis, Conceptualization.

Declaration of competing interest

The authors declare that they have no known competing financial interests or personal relationships that could have appeared to influence the work reported in this paper.

Acknowledgement

We gratefully acknowledge Kimberley Boagey, Food Laboratory Technician at Teesside University, for her invaluable support to our MSc students during the completion of their research projects.

Data availability

Data will be made available on request.

References

A, S., Venkatachalam, S., John, S.G., Kuppuswamy, K., 2015. Foam mat drying of food materials: a review. J. Food Process. Preserv. 39, 3165–3174.
Aghajanzadeh, S., Ziaiifar, A.M., Verkerk, R., 2023. Effect of thermal and non-thermal treatments on the color of citrus juice: A review. Food Rev. Int. 39 (6), 3555–3577.
Akbarbaglu, Z., Mazloomi, N., Sarabandi, K., Ramezani, A., Khaleghi, F., Hamzehkollaei, A.R., Jafari, S.M., Hesarinejad, M.A., 2024. Stabilization of antioxidant thyme-leaves extract (Thymus vulgaris) within biopolymers and its application in functional bread formulation. Future Foods 9, 100356.
AL-Ibraheemi, Z.A.M.S.A.M.S.T.F., I, A.M.C.M.T.S., Mahdi, A.B., 2013. Deformation and mechanical characteristics of compacted binary mixtures of plastic (microcrystalline cellulose), elastic (sodium starch glycolate), and brittle (Lactose monohydrate) pharmaceutical excipients. Part. Sci. Technol. 31, 561–567.
AL-Muhtaseb, A.H., Mcminn, W.A.M., Magee, T.R.A., 2002. Moisture sorption isotherm characteristics of food products: a review. Food Bioprod. Process. 80, 118–128.
Allen, K.E., Dickinson, E., Murray, B., 2006. Acidified sodium caseinate emulsion foams containing liquid fat: a comparison with whipped cream. LWT - Food Sci. Technol. (Lebensmittel-Wissenschaft -Technol.) 39, 225–234.
Amin, M.C., Fell, J.T., 2004. Comparison studies on the percolation thresholds of binary mixture tablets containing excipients of plastic/brittle and plastic/plastic deformation properties. Drug Dev. Ind. Pharm. 30, 937–945.
Bhusari, S.N., Muzaffar, K., Kumar, P., 2014. Effect of carrier agents on physical and microstructural properties of spray dried tamarind pulp powder. Powder Technol. 266, 354–364.
Bonilla, E., Azuara, E., Beristain, C.I., Vernon-Carter, E.J., 2010. Predicting suitable storage conditions for spray-dried microcapsules formed with different biopolymer matrices. Food Hydrocoll. 24, 633–640.
Čakarević, J., Šeregelj, V., Tumbas Šaponjac, V., Ćetković, G., Čanadanović Brunet, J., Popović, S., Kostić, M.H., Popović, L., 2020. Encapsulation of beetroot juice: a study on the application of pumpkin oil cake protein as new carrier agent. J. Microencapsul. 37, 121–133.
Carmo, E.L.D., Teodoro, R.A.R., Félix, P.H.C., Fernandes, R.V.D.B., Oliveira, É.R.D., Veiga, T.R.L.A., Borges, S.V., Botrel, D.A., 2018. Stability of spray-dried beetroot extract using oligosaccharides and whey proteins. Food Chem. 249, 51–59.
Carr, R.L., 1965. Classifying Flow Properties of Solids.
Chandrakar, N., Padhi, S., Saraugi, S.S., Sehrawat, R., Singh, A., Routray, W., 2024. Whey protein and maltodextrin conjugated foam-mat dried honey powder: functional, physicochemical, structural, rheological and thermal characterization. Chem. Eng. Res. Des. 209, 367–379.
Chen, W., Hadde, E.K., Chen, J., 2021. Development of a ball back extrusion technique for texture analysis of fluid food. J. Texture Stud. 52, 461–469.
Dabestani, M., Yeganehzad, S., 2019. Effect of Persian gum and Xanthan gum on foaming properties and stability of pasteurized fresh egg white foam. Food Hydrocoll. 87, 550–560.
Darniadi, S., Ho, P., Murray, B.S., 2018. Comparison of blueberry powder produced via foam-mat freeze-drying versus spray-drying: evaluation of foam and powder properties. J. Sci. Food Agric. 98, 2002–2010.
Dehghannya, J., Pourahmad, M., Ghanbarzadeh, B., Ghaffari, H., 2018a. Heat and mass transfer modeling during foam-mat drying of lime juice as affected by different ovalbumin concentrations. J. Food Eng. 238, 164–177.
Dehghannya, J., Pourahmad, M., Ghanbarzadeh, B., Ghaffari, H., 2018b. Influence of foam thickness on production of lime juice powder during foam-mat drying: experimental and numerical investigation. Powder Technol. 328, 470–484.
Dickinson, E., 1992. An Introduction to Food Colloids/Eric Dickinson. Oxford University Press, Oxford ; New York.
Dickinson, E., 2011. Mixed biopolymers at interfaces: competitive adsorption and multilayer structures. Food Hydrocoll. 25, 1966–1983.
Fang, Y., Selomulya, C., Chen, X.D., 2007. On measurement of food powder reconstitution properties. Dry. Technol. 26, 3–14.
Farshchi, A., Hassanpour, A., Ettelaie, R., Bayly, A.E., 2019. Evolution of surface microstructure and moisture sorption characteristics of spray-dried detergent powders. J. Colloid Interface Sci. 551, 283–296.
Farshchi, A., Hassanpour, A., Tantawy, H., Bayly, A.E., 2022. Effect of matrix composition on the flowability of spray-dried detergent powders. Adv. Powder Technol. 33, 103433.
García-Segovia, P., Igual, M., Martínez-Monzó, J., 2021. Beetroot microencapsulation with pea protein using spray drying: physicochemical, structural and functional properties. Appl. Sci. 11, 6658.
Hajiaghaei, M., Sharifi, A., 2022. Physicochemical properties of red beetroot and quince fruit extracts instant beverage powder: effect of drying method and maltodextrin concentration. J. Food Qual. 2022, 7499994.
Hardy, Z., Jideani, V.A., 2017. Foam-mat drying technology: a review. Crit. Rev. Food Sci. Nutr. 57, 2560–2572.
Hausner, H.H., 1967. Friction Conditions in a Mass of Metal Powder. Polytechnic Inst. of Brooklyn. Univ., of California, Los Angeles.
Islam, M.Z., Jahan, M.I., Monalisa, K., Rana, R., Hoque, M.M., 2024. Impact of maltodextrin, egg white protein addition and microwave-assisted foam mat drying on drying kinetics, microstructures, physicochemical and quality attributes of jackfruit juice powder. LWT 200, 116158.
Janiszewska, E., 2014. Microencapsulated beetroot juice as a potential source of betalain. Powder Technol. 264, 190–196.
Jurić, S., Jurić, M., Król-Kilińska, Ż., Vlahoviček-Kahlina, K., Vinceković, M., Dragović-Uzelac, V., Donsì, F., 2022. Sources, stability, encapsulation and application of natural pigments in foods. Food Rev. Int. 38, 1735–1790.
Kalajahi, S.G., Malekjani, N., Samborska, K., Akbarbaglu, Z., Gharehbeglou, P., Sarabandi, K., Jafari, S.M., 2023. Encapsulated powders of Alcea flower polyphenol-rich extract by different hydrocolloid carriers: characterisation, antioxidant activity and chemical structures. Int. J. Food Sci. Technol. 58, 4246–4255.
Kandasamy, S., Naveen, R., 2022. A review on the encapsulation of bioactive components using spray-drying and freeze-drying techniques. J. Food Process. Eng. 45, e14059.
Kawakita, K., Lüdde, K.-H., 1971. Some considerations on powder compression equations. Powder Technol. 4, 61–68.
Kerr, W.L., Varner, A., 2020. Chemical and physical properties of vacuum-dried red beetroot (Beta vulgaris) powders compared to other drying methods. Dry. Technol. 38, 1165–1174.
Khomane, K.S., More, P.K., Raghavendra, G., Bansal, A.K., 2013. Molecular understanding of the compaction behavior of Indomethacin polymorphs. Mol. Pharm. 10, 631–639.
Kulkarni, S.S., Janssen, P.H.M., Dickhoff, B.H.J., 2023. The impact of material chemistry and morphology on attrition behavior of excipients during high shear blending. Powder Technol. 427, 118694.
Lebrun, P., Krier, F., Mantanus, J., Grohganz, H., Yang, M., Rozet, E., Boulanger, B., Evrard, B., Rantanen, J., Hubert, P., 2012. Design space approach in the optimization of the spray-drying process. Eur. J. Pharm. Biopharm. 80, 226–234.
Maciel, K.S., Teixeira, L.J.Q., Lucia, S.M.D., Saraiva, S.H., 2022. Optimization of foam mat drying for instant coffee processing and its effect on drying kinetics and quality characteristics. Dry. Technol. 40, 1866–1880.
Martínez-Padilla, L.P., García-Rivera, J.L., Romero-Arreola, V., Casas-Alencáster, N.B., 2015. Effects of xanthan gum rheology on the foaming properties of whey protein concentrate. J. Food Eng. 156, 22–30.
Mehrali, P., Peighambardoust, S.H., Akbarmehr, A., Sarabandi, K., 2025. Insights into selection and application of carbohydrate-based carriers for microencapsulation: stability and functional properties of maltodextrin, gum Arabic, and β-cyclodextrin in encapsulating tea flower pollen peptides. Carbohydr. Polym. Technol. Appl. 9, 100700.
Minor, M., Vingerhoeds, M.H., Zoet, F.D., DE Wijk, R., VAN Aken, G.A., 2009. Preparation and sensory perception of fat-free foams – effect of matrix properties and level of aeration. Int. J. Food Sci. Technol. 44, 735–747.

Mohanan, A., Nickerson, M.T., Ghosh, S., 2020. Utilization of pulse protein-xanthan gum complexes for foam stabilization: the effect of protein concentrate and isolate at various pH. Food Chem. 316, 126282.
Mosquera, L.H., Moraga, G., Martínez-Navarrete, N., 2012. Critical water activity and critical water content of freeze-dried strawberry powder as affected by maltodextrin and Arabic gum. Food Res. Int. 47, 201–206.
Mounir, S., 2017. Foam Mat Drying. *Drying Technologies for Foods-Fundamentals and Applications*, pp. 169–191.
Murray, B.S., 2007. Stabilization of bubbles and foams. Curr. Opin. Colloid Interface Sci. 12, 232–241.
Murray, B.S., 2020. Recent developments in food foams. Curr. Opin. Colloid Interface Sci. 50, 101394.
Murray, B.S., Ettelaie, R., 2004. Foam stability: proteins and nanoparticles. Curr. Opin. Colloid Interface Sci. 9, 314–320.
Muthukumaran, A., Ratti, C., Raghavan, V.G.S., 2008. Foam-Mat freeze drying of egg white and mathematical modeling part I optimization of egg white Foam stability. Dry. Technol. 26, 508–512.
Naji-Tabasi, S., Emadzadeh, B., Shahidi-Noghabi, M., Abbaspour, M., Akbari, E., 2021. Physico-chemical and antioxidant properties of barberry juice powder and its effervescent tablets. Chem. biol. technol. agric 23 (8).
Narchi, I., Vial, C., Djelveh, G., 2009. Effect of protein–polysaccharide mixtures on the continuous manufacturing of foamed food products. Food Hydrocoll. 23, 188–201.
Ng, M.L., Sulaiman, R., 2018. Development of beetroot (Beta vulgaris) powder using foam mat drying. LWT 88, 80–86.
Ninfali, P., Angelino, D., 2013. Nutritional and functional potential of Beta vulgaris cicla and rubra. Fitoterapia 89, 188–199.
Nooshkam, M., Varidi, M., Alkobeisi, F., 2022. Bioactive food foams stabilized by licorice extract/whey protein isolate/sodium alginate ternary complexes. Food Hydrocoll. 126, 107488.
Nordström, J., Welch, K., Frenning, G., Alderborn, G., 2008. On the physical interpretation of the Kawakita and Adams parameters derived from confined compression of granular solids. Powder Technol. 182, 424–435.
Nsengiyumva, E.M., Alexandridis, P., 2022. Xanthan gum in aqueous solutions: fundamentals and applications. Int. J. Biol. Macromol. 216, 583–604.
Omidi, S., Aarabi, A., Zaki Dizaji, H., Shahdadi, F., 2024. Microwave-assisted foam mat drying of red beet pulp: influence of milk protein concentrate (MPC) and maltodextrin as a foaming agent, optimization and quality attribute. J. Food Meas. Char. 18, 2505–2525.
Ong, M.Y., Yusof, Y.A., Aziz, M.G., Chin, N.L., Amin, N.A.M., 2014. Characterisation of fast dispersible fruit tablets made from green and ripe mango fruit powders. J. Food Eng. 125, 17–23.
Ouyang, J., Wang, J., Wang, Y., Yin, Q., Hao, H., 2015. Thermodynamic study on dynamic water and organic vapor sorption on amorphous valnemulin hydrochloride. Front. Chem. Sci. Eng. 9, 94–104.
Ozcelik, M., Ambros, S., Morais, S.I.F., Kulozik, U., 2020. Storage stability of dried raspberry foam as a snack product: effect of foam structure and microwave-assisted freeze drying on the stability of plant bioactives and ascorbic acid. J. Food Eng. 270, 109779.
Pitalua, E., Jimenez, M., Vernon-Carter, E.J., Beristain, C.I., 2010. Antioxidative activity of microcapsules with beetroot juice using gum Arabic as wall material. Food Bioprod. Process. 88, 253–258.
Qadri, O.S., Srivastava, A.K., Yousuf, B., 2020. Trends in foam mat drying of foods: special emphasis on hybrid foam mat drying technology. Crit. Rev. Food Sci. Nutr. 60, 1667–1676.
Raikos, V., Campbell, L., Euston, S.R., 2007. Effects of sucrose and sodium chloride on foaming properties of egg white proteins. Food Res. Int. 40, 347–355.
Ravichandran, K., Palaniraj, R., Saw, N.M.M.T., Gabr, A.M., Ahmed, A.R., Knorr, D., Smetanska, I., 2014. Effects of different encapsulation agents and drying process on stability of betalains extract. J. Food Sci. Technol. 51, 2216–2221.
Ray, S., Raychaudhuri, U., Chakraborty, R., 2016. An overview of encapsulation of active compounds used in food products by drying technology. Food Biosci. 13, 76–83.
Ren, Y., Jia, F., Li, D., 2024. Ingredients, structure and reconstitution properties of instant powder foods and the potential for healthy product development: a comprehensive review. Food Funct. 15, 37–61.
Sadahira, M.S., Rodrigues, M.I., Akhtar, M., Murray, B.S., Netto, F.M., 2018. Influence of pH on foaming and rheological properties of aerated high sugar system with egg white protein and hydroxypropylmethylcellulose. LWT 89, 350–357.
Saifullah, M., Yusof, Y.A., Chin, N.L., Aziz, M.G., 2016. Physicochemical and flow properties of fruit powder and their effect on the dissolution of fast dissolving fruit powder tablets. Powder Technol. 301, 396–404.
Saifullah, M., Yusof, Y.A., Chin, N.L., Aziz, M.G., Mohammed, M.A.P., Aziz, N.A., 2014. Tableting and dissolution characteristics of mixed fruit powder. Agric. & Agric. Sci. Procedia 2, 18–25.
Sanderson, G.R., 1981. Applications of Xanthan gum. Br. Polym. J. 13, 71–75.
Seerangurayar, T., Manickavasagan, A., AL-Ismaili, A.M., AL-Mulla, Y.A., 2017. Effect of carrier agents on flowability and microstructural properties of foam-mat freeze dried date powder. J. Food Eng. 215, 33–43.
Shakir, B.K., Simone, V., 2024. Estimation of betalain content in beetroot peel powder. Ital. J. Food Sci. 36, 53.
Siddiqui, A., Nazzal, S., 2007. Measurement of surface color as an expedient QC method for the detection of deviations in tablet hardness. Int. J. Pharm. 341, 173–180.
Stapley, A., 2008. 12 freeze drying. Frozen food science and technology 248.
Steendam, R., Frijlink, H.W., Lerk, C.F., 2001. Plasticisation of amylodextrin by moisture. Consequences for compaction behaviour and tablet properties. Eur. J. Pharmaceut. Sci. 14, 245–254.
Sun, J., Chang, C., Su, Y., Gu, L., Yang, Y., Li, J., 2022. Impact of saccharides on the foam properties of egg white: correlation between rheological, interfacial properties and foam properties. Food Hydrocoll. 122, 107088.
Tekin, İ., Özcan, K., Ersus, S., 2023. Optimization of ionic gelling encapsulation of red beet (Beta vulgaris L.) juice concentrate and stability of betalains. Biocatal. Agric. Biotechnol. 51, 102774.
Wu, S., Yuan, Y., Yin, J., Hu, H., Pei, H., Li, W., Zhang, X., 2022. Characteristics of effervescent tablets of Aronia melanocarpa: response surface design and antioxidant activity evaluation. J. Food Meas. Char. 16, 2969–2977.
Wyatt, N.B., Liberatore, M.W., 2009. Rheology and viscosity scaling of the polyelectrolyte xanthan gum. J. Appl. Polym. Sci. 114, 4076–4084.
Xu, Y., Yang, N., Yang, J., Hu, J., Zhang, K., Nishinari, K., Phillips, G.O., Fang, Y., 2020. Protein/polysaccharide intramolecular electrostatic complex as superior food-grade foaming agent. Food Hydrocoll. 101, 105474.
Yang, X., Foegeding, E.A., 2011. The stability and physical properties of egg white and whey protein foams explained based on microstructure and interfacial properties. Food Hydrocoll. 25, 1687–1701.
Zea, L.P., Yusof, Y.A., Aziz, M.G., Ling, C.N., Amin, N.A.M., 2013. Compressibility and dissolution characteristics of mixed fruit tablets made from guava and pitaya fruit powders. Powder Technol. 247, 112–119.